JOURNAL OF SOLID STATE CHEMISTRY 97, 249–256 (1992)

Characterization of the Single Phase Region with Spinel Structure in the Ternary System In_2S_3–FeS–FeS_2

MANFRED WOMES,*† JOSETTE OLIVIER-FOURCADE,* JEAN-CLAUDE JUMAS,* FRANK AUBERTIN,† AND ULRICH GONSER†

*Laboratoire de Physicochimie des Matériaux (URA D0407 CNRS), Université Montpellier II- Sciences et Techniques du Languedoc, Place Eugène Bataillon, 34095 Montpellier Cédex 5, France; and †Werkstoffwissenschaften, Universität des Saarlandes, D6600 Saarbrücken, Germany

Received June 6, 1991; in revised form September 23, 1991

The limit of single-phase solid solubility in a spinel host lattice in the system In_2S_3–FeS–FeS_2 has been determined. Mössbauer spectroscopy showed that all iron is bivalent and, for the major part, occupies the *B*-sites (δ = 0.81–0.89 mm/s, Δ = 3.16–3.25 mm/s). The fraction of tetrahedral iron depends on the sample composition and the thermal treatment. Mössbauer spectroscopy also showed the influence of tetrahedral vacancies by causing quadrupole splittings on tetrahedral subspectra (δ = 0.64–0.74 mm/s and Δ = 0.55–1.07 mm/s). © 1992 Academic Press, Inc.

Introduction

Spinel-type solid solutions based on the host lattice of In_2S_3 (*1*) have attracted considerable interest in recent years (*2–5*). The binary system In_2S_3–FeS was studied in detail by Rustamov *et al.* (*2*) using X-ray diffraction, D.T.A., electrical conductivity, and microhardness measurements. They found a linear variation of the cubic lattice constant from 10.72 Å for pure In_2S_3 to 10.52 Å for the limit of solubility containing 55 mole% FeS in the spinel lattice. From the electric conductivity of their samples Rustamov *et al.* (*2*) conclude that Fe should be bivalent in this material. In our investigation we used Mössbauer spectroscopy in order to confirm their conclusion and to extend the study to the ternary In_2S_3–FeS–FeS_2 system.

Three modifications of In_2S_3 are known (*6*). The low temperature β-form is derived from the spinel structure. It consists of cubic close-packed sulfur anions with In^{3+} cations on all octahedral (B) sites and $\frac{2}{3}$ of the tetrahedral (A) sites. The remaining vacant tetrahedral sites are ordered into 4_1 screws along the *c*-direction. At 420°C a transition leading to the α-form with randomly arranged tetrahedral vacancies is observed. The α–γ transition from the cubic α-form to the tetragonal γ-form occuring at 754°C is accompanied by a change of all tetrahedral In to octahedral sites. This transition is reversible in pure In_2S_3, so that the pure γ-form is not stable below the transition temperature. However, small amounts of As or Sb can

0022-4596/92 $3.00

block this transition, so that the γ-form can be observed even at room temperature.

The stoichiometric iron monosulfide FeS has the hexagonal NiAs structure (*7*) in which both Fe and S form slightly distorted hexagonal sublattices. The disulfide FeS_2 shows the simple cubic structure of face-centered NaCl with $(S–S)^{2-}$-pairs on the anion positions ordered equally along the four [1 1 1] cube directions (*8*). The S–S distance in these pairs is 2.15 Å, which is considerably less than the S–S distances in pure In_2S_3 of 3.6–3.9 Å or in FeS of 3.30–3.71 Å.

Experimental

The binary sulfides In_2S_3, FeS, and FeS_2 have been synthesized by heating stoichiometric powder mixtures of the pure elements in evacuated and sealed silica tubes (to 450°C in the case of FeS_2 and to 800°C in all other cases).

The ternary samples were prepared from finely ground stoichiometric mixtures of the binary sulfides by firing them under vacuum to 550°C (120 h.) and subsequently to 800°C (170 h.) followed by quenching in cold water. Additionally, some samples were synthesized from the elements at 680°C (200 h.) and thereafter cooled slowly to room temperature. The purities of the binary sulfides as well as the structures and lattice constants of our samples were checked by X-ray powder diffraction.

X-ray powder diffraction patterns have been recorded with Cu$K\alpha$ radiation on a Philips powder diffractometer controlled by a microcomputer.

Mössbauer spectra have been recorded in standard transmission geometry using a ^{57}Co*Rh* source. All isomer shift values are given with respect to the center of an α-Fe spectrum at room temperature.

Results

All samples have first been examined by X-ray diffraction. In the binary system

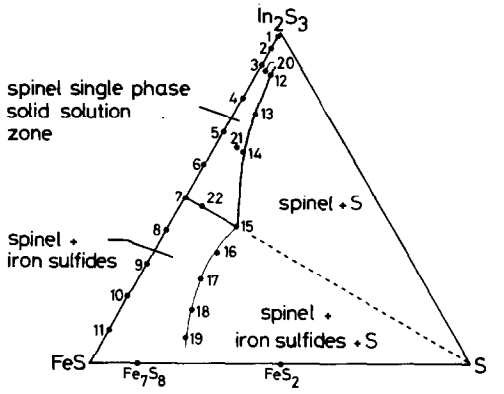

FIG. 1. Representation of the sample compositions as determined from the measured sulfur excess in the ternary system In_2S_3–FeS–S. The samples have been numbered 1 to 22.

In_2S_3–FeS the limit of single phase solid solubility was found between 40 and 50 mole% of In_2S_3, in agreement with the 45 mole% found by Rustamov *et al.* (*2*, *3*). Figure 1 shows their positions in an In_2S_3–FeS–S phase diagram where they are numbered 1–11. The samples within the limit of solid solubility (numbers 1–7) crystallized in the spinel lattice based on the cubic α-form of In_2S_3; samples outside the limit (numbers 8–11) exhibited impurities of FeS. Figure 2a shows as an example the Mössbauer spectrum of a sample prepared from 20 mole% In_2S_3 and 80 mole% FeS (number 10). It consists of a doublet, which is due to the spinel phase, and the typical six-line pattern of stoichiometric FeS.

All samples of the system In_2S_3–FeS_2 showed deposits of elementary sulfur in the tubes after reaction. The amounts of these deposits depend on the FeS_2 fraction and lie between 30 and 45% of the sulfur previously bonded in FeS_2, which can be explained by the decomposition of FeS_2 to FeS_{1+x} and sulfur,

$$FeS_2 \rightarrow FeS_{1+x} + (1 - x)\,S,$$

where in our case $0.10 \leq x \leq 0.40$. Such a

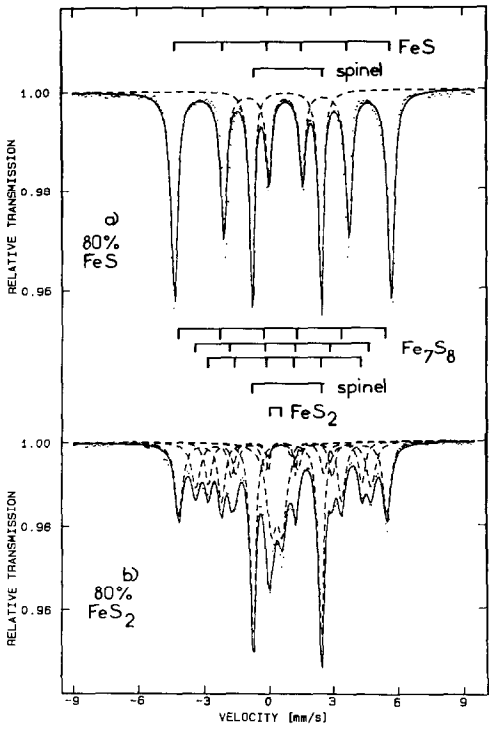

FIG. 2. Room temperature Mössbauer spectra of samples outside the single-phase solid solubility zone prepared with an excess of FeS (a) or FeS_2 (b).

decomposition is necessary since the S–S distance of 2.15 Å of the $(S_2)^{2-}$ anions in FeS_2 is too small to allow these sulfur pairs to enter into the spinel structure. However, neither X-ray diffraction nor Mössbauer spectroscopy gave any indication of a reaction pathway of the excess sulfur contained in FeS_{1+x} compared to pure FeS. Variation of the FeS_2 : FeS ratio at constant In_2S_3 percentage had no influence on the X-ray spectra; also, no traces of Fe^{3+} or $(S_2)^{2-}$ pairs were found by Mössbauer spectroscopy in the form of changes in quadrupole splittings or line broadenings.

If we suppose that FeS_{1+x} has entered into the spinel lattice instead of FeS_2, the limit of the solid solution region should be represented on the basis of a ternary system In_2S_3–FeS–S as it is shown in Fig. 1. The positions of the In_2S_3–FeS_2 samples in this phase diagram (numbers 12–19) have been determined from the measured sulfur deposits found in the tubes after reaction. The limit of solid solubility was equally found between 40 and 50 mole% of In_2S_3. Samples outside the single phase solid solution region (numbers 16–19) contain impurities of Fe_7S_8 and FeS_2. Figure 2b shows the Mössbauer spectrum of a sample prepared from 20 mole% In_2S_3 and 80 mole% FeS_2 (number 18). Three subspectra can be distinguished: the spinel phase, FeS_2, and three six-line hyperfine patterns whose isomer shifts and quadrupole splittings are typical for pyrrhotite, Fe_7S_8, at room temperature (*9*, *10*), which confirms the decomposition reaction given above.

Additionally, a series of samples with a constant FeS_2 : FeS ratio of 1 : 1 has been prepared. As before, 30–45% of the sulfur bonded in FeS_2 is lost as deposits in the tubes, and the limit of solid solubility is found at 40–50 mole% of In_2S_3 (numbers 20–22). Thus, the limit of single phase solid solution only depends on the In : Fe ratio. Figure 3 shows the variation of the lattice parameter with the In_2S_3 concentration in the system In_2S_3–FeS. X-ray powder diffraction revealed no influence of the

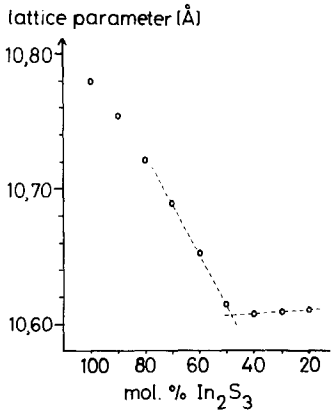

FIG. 3. Variation of the lattice parameter as a function of the In_2S_3 concentration in the In_2S_3–FeS system.

FeS_2 : FeS ratio on linewidths, intensities, or the lattice parameters. On the other hand, the observed variations of the line intensities with changes in the In : Fe ratio agree with theoretical spectra calculated on the basis of random occupation of octahedral sites by Fe and In, and filling of structural vacancies on tetrahedral sites by In.

The Mössbauer absorption spectra of all quenched samples within the single phase solid solution zone consist of one dominant doublet and several partially unresolved secondary doublets. Figure 4 shows the spectra obtained in the In_2S_3–FeS system. The isomer shifts of the main doublet vary from 0.81 to 0.89 mm/sec, and the quadrupole splittings lie between 3.16 and 3.25 mm/sec. Linewidths of 0.26–0.30 mm/sec are found, except for the samples prepared from 70 mole% In_2S_3 and 30 mole% iron sulfides, where the line widths are 0.34–0.44 mm/sec (numbers 5, 14, 21). No significant variation of these parameters with composition can be observed. The values are typical for high-spin Fe^{2+} on octahedral sites and agree well with those found by other authors for $FeIn_2S_4$ (*11–13*). At low iron concentration the main doublet shows asymmetry, with a broader, less intense, low-velocity line and a sharper high-velocity line of equal area fraction. This asymmetry decreases as the iron content increases, and a completely symmetric doublet is observed if the total concentration of iron sulfides is higher than 20 mole%. The Mössbauer parameters of the secondary doublets depend strongly on the composition. In a first attempt the subspectra have been fitted roughly as one broad quadrupole doublet in order to obtain mean values $\bar{\delta}$ and $\overline{\Delta E_q}$ of the isomer shifts and quadrupole splittings. As can be seen from Fig. 5, $\overline{\Delta E_q}$ increases from 0.55 to 1.07 mm/sec with increasing iron content, while the mean isomer shift $\bar{\delta}$ is not affected and varies between 0.64 and 0.74 mm/sec.

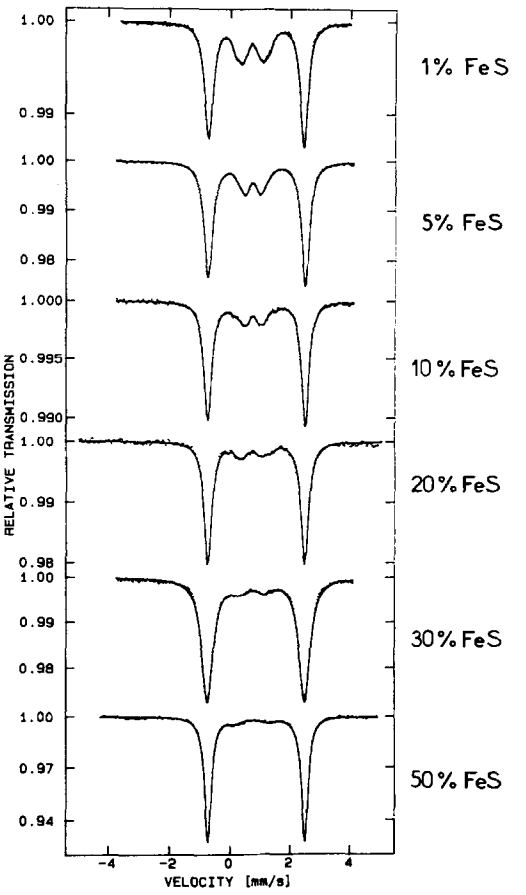

FIG. 4. Room temperature Mössbauer spectra of quenched samples prepared from mixtures of In_2S_3 and FeS. Concentrations given in mole%. Secondary doublets have fitted to three and six doublets in the case of 1 and 5% FeS, respectively, as explained in the text, and to one large doublet in all other cases.

From those mean values $\bar{\delta}$ and $\overline{\Delta E_q}$ we conclude that the secondary doublets are due to high-spin Fe^{2+} on tetrahedral sites rather than Fe^{3+}, in agreement with crystallographic investigations by Hill *et al.* (*14*), who reported about 5% iron on tetrahedral sites in $FeIn_2S_4$, and Mössbauer studies of this compound by Riedel and Karl (*13*). The area fraction decreases from 33 to 7% as the total concentration of iron sulfides is raised from 1 to 50

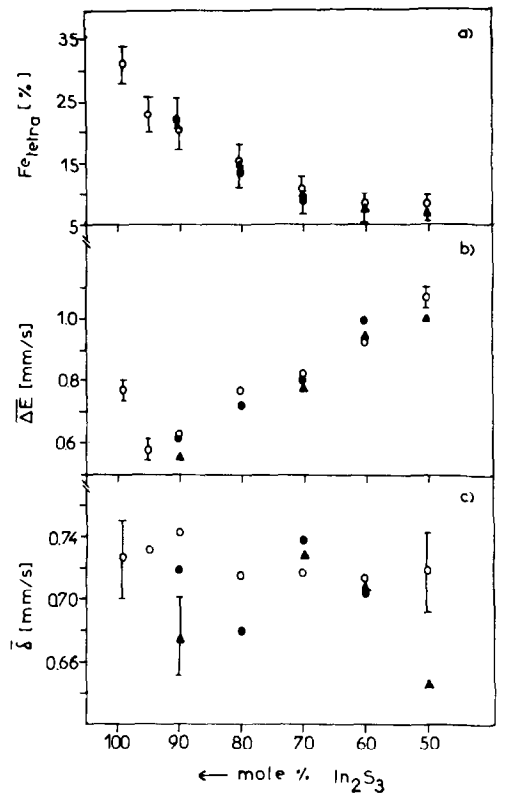

FIG. 5. Variation of tetrahedral iron fraction (a), mean quadrupole splitting ΔE_q (b) and mean isomer shift δ (c) of the secondary subspectra with composition for the systems: ○, In_2S_3–FeS; ●, In_2S_3–FeS_2; ▲, In_2S_3–FeS–FeS_2. Error bars have been omitted where they do not change over the whole composition range.

mole%. This decrease reflects the gradual filling of structural tetrahedral vacancies in the spinel lattice mainly by In atoms. As the amount of iron in *B*-sites is raised, more and more indium changes from octahedral to tetrahedral positions. Thus, the concentration of tetrahedral vacancies (which could be alternatively occupied by iron) is gradually reduced from $\frac{8}{3}$ per unit cell in pure In_2S_3 to zero in $FeIn_2S_4$.

To obtain more satisfying fits of the secondary doublets, we considered all possible arrangements of nearest and next-nearest neighbors of a tetrahedral site and calculated the probabilities of each of them. Fe^{2+} on *A*-sites is bonded to four sulfur anions which, in turn, are bonded each to three metal cations on *B*-sites. These can be (3 In), (2 In + 1 Fe), (1 In + 2 Fe), or (3 Fe) which leads to 35 different arrangements of these next-nearest octahedral neighbors of an *A*-site. Additionally, the four nearest tetrahedral sites have to be taken into account. The $Fe_{tet.}$–$Fe_{tet.}$ distances (4.60 Å) are slightly longer than the $Fe_{tet.}$–$Fe_{oct.}$ distances (4.40 Å) (*14*), so that tetrahedral sites represent the third neighboring shell. These sites can be occupied by Fe or In, or can be vacant (□) leading to 15 different possible arrangements. The general distribution of the cations and vacancies on the different sites can be written as

$$(Fe^{2+}_{\lambda}\ In^{3+}_{2/3+y/3-\lambda}\ \square_{1/3-y/3})\ [Fe^{2+}_{y-\lambda}\ In^{3+}_{2-y+\lambda}]\ S^{2-}_{4},$$

where y is the number of iron atoms per one-eighth of the unit cell and varies from zero for In_2S_3 to unity for $FeIn_2S_4$, and λ gives the number of tetrahedral iron and lies between zero and y. λ can be calculated from the areas of main and secondary doublets using the value of $f_o/f_t = 0.94$ for the Debye–Waller factors of octahedral (f_o) and tetrahedral (f_t) iron in Fe_3O_4 (*15*). In the case of sample 1 (1% FeS), 31% of all iron is on tetrahedral sites which leads to $y = 0.02$ and $\lambda = 6.2 \times 10^{-3}$. Calculating now the probabilities of each of the 35 octahedral arrangements we find that only the one consisting of 4 × (3 In) is important (probability $p = 0.92$), while we have to deal with three different tetrahedral environments: 4 In ($p = 0.20$), 3 In + 1 □ ($p = 0.39$), and 2 In + 2 □ ($p = 0.29$). Thus, the secondary subspectra have to be fitted to three doublets with quadrupole splittings increasing from 4 In to 2 In + 2 □. In the fit, the linewidths have been constrained to be equal and the peak heights to be in the ratio 2 : 4 : 3. This leads

to the following values of isomer shifts and quadrupole splittings:

	δ (mm/sec)	ΔE_q (mm/sec)
4 In	0.73	0.36
3 In + 1 □	0.73	0.71
2 In + 2 □	0.74	1.14

The linewidth of 0.30 mm/sec is still in the usual range, which indicates that no further subspectrum has to be added. The fact that even in the completely symmetric case of 4 $In_{tet.}$ and 12 $In_{oct.}$ a quadrupole split doublet is observed reflects a slight deviation from the ideal tetrahedral symmetry. Since we considered just the first sphere of tetrahedral sites in our calculation, this distortion might be due to vacancies in the second and outer spheres. In the case of sample 2 (5% FeS) the same three tetrahedral environments are important, although their probabilities are slightly changed (4 In, $p = 0.21$; 3 In + 1 □, $p = 0.37$; 2 In + 2 □, $p = 0.25$). But in contrast to sample 1, now two different octahedral arrangements have to be considered: 4 × (3 In), $p = 0.63$, and 3 × (3 In) + (2 In + 1 Fe), $p = 0.30$. Thus, the secondary subspectrum has to be fitted to six doublets if we disregard all the possible arrangements of the octahedral iron atom relative to the tetrahedral vacancies, iron, or indium atoms. Three of these six doublets should be the same as for sample 1, each of them accompanied by one further doublet of about half intensity and a slightly higher quadrupole splitting representing the presence of one iron atom on one of the twelve surrounding *B*-sites. However, it was not possible to obtain a satisfying fit by constraining the isomer shifts and quadrupole splittings of three of the doublets to the values found for composition 1 and their intensities to the values theoretically expected for sample 2. A proper fit to six doublets with the calculated intensities could be obtained by allowing somewhat smaller quadrupole splittings:

	ΔE_q (mm/sec)		ΔE_q (mm/sec)
4 $In_{tet.}$ + 12 $In_{oct.}$	0.33	4 $In_{tet.}$ + 11 $In_{oct.}$ + 1 $Fe_{oct.}$	0.37
3 $In_{tet.}$ + $□_{tet.}$ + 12 $In_{oct.}$	0.51	3 $In_{tet.}$ + $□_{tet.}$ + 11 $In_{oct.}$ + 1 $Fe_{oct.}$	0.65
2 $In_{tet.}$ + 2 $□_{tet.}$ + 12 $In_{oct.}$	0.96	2 $In_{tet.}$ + 2 $□_{tet.}$ + 11 $In_{oct.}$ + 1 $Fe_{oct.}$	0.98

If our previous assumption holds, that the quadrupole splittings are partially due to vacancies in the next-nearest and outer spheres of tetrahedral sites, slightly reduced ΔE_q's in the case of composition 2 compared to 1 seem to be reasonable since the concentration of vacancies also is reduced.

Considering now composition 3 (10% FeS) we find that the three most important tetrahedral environments have to be combined with three octahedral arrangements: 4 × (3 In), $p = 0.37$; 3 × (3 In) + (2 In + 1 Fe), $p = 0.38$, and 2 × (3 In) + 2 × (2 In + 1 Fe), $p = 0.15$, so that in principle a total of nine doublets has to be included in the fit. As the intensity and resolution of the secondary subspectra of this and all following samples of higher iron concentration decreases, no further fits to the structural details have been tried.

Anyhow, our approach seems to be justified since the mean quadrupole splitting $\overline{\Delta E_q}$ in Fig. 5b reflects well the tendency to less symmetric octahedral arrangements with increasing iron content which, however, is partially balanced by the increasing probability of the symmetric tetrahedral 4 In-environment.

These secondary doublets are of much weaker intensity or even absent if the sample is cooled slowly. Figure 6 shows the Mössbauer spectra of a quenched (a) and slowly cooled (b) sample of the composition 6 (20% FeS). It is known from the work

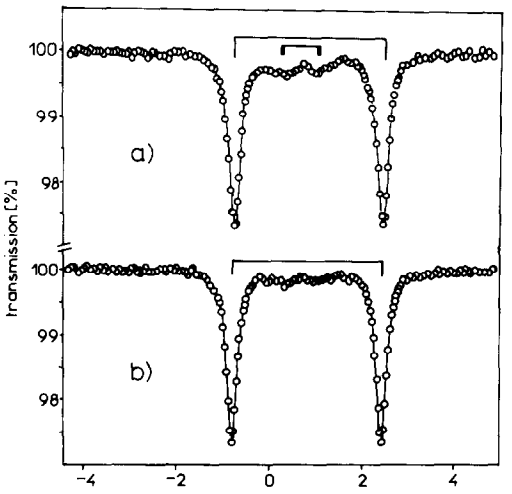

FIG. 6. Room temperature Mössbauer spectra of a quenched (a) and slowly cooled (b) sample of 20 mole% FeS and 80 mole% In_2S_3.

of Hafner and Laves (*16*) on $MgAl_2O_4$ and $LiAl_5O_8$ that the cation distribution on octahedral and tetrahedral sites in spinels depends on the thermal treatment and tends to a higher degree of disorder if the temperature of sample preparation is raised. Thus, Fe^{2+} on tetrahedral sites represents a high-temperature form which can be preserved by quenching or reconverted to the low-temperature form with all iron on *B*-sites by slow cooling. Samples kept at room temperature for several months after preparation showed no transition of tetrahedral iron to *B*-sites with time by changes of the area fractions.

The reason of the asymmetry of the main doublet of octahedral iron has not yet been determined. Since this asymmetry decreases as the iron concentration increases, we suppose that the asymmetry reflects the influence of tetrahedral vacancies on the *B*-sites. However, to clarify this point, temperature-dependent Mössbauer spectroscopy should be carried out to distinguish between relaxation phenomena or a possible Goldanskii–Karyagin effect.

Conclusions

The limit of the single-phase solid solubility in the ternary system In_2S_3–FeS–FeS_2 has been determined by X-ray diffraction and Mössbauer spectroscopy. It has been shown that FeS_2 decomposes to FeS_{1+x} and $(1 - x)$ S and that FeS_{1+x} can be entered into the spinel structure with $0.1 \leq x \leq 0.4$. Mössbauer spectroscopy showed all iron to be bivalent and to occupy mainly octahedral sites. The structural vacancies on the tetrahedral sites of the spinel structure could be detected directly via quadrupole splittings of the subspectra of tetrahedral iron, even in the case of symmetrical environments of nearest octahedral and next-nearest tetrahedral neighbors.

For more detailed informations on the influence of the vacancies a series of temperature-dependent spectra should be carried out.

Acknowledgments

The authors thank MAE (France)–DAAD (Germany) for the scholarship under the auspices of the PROCOPE project. We are grateful to Dr. R. Fourcade for support in X-ray studies and fruitful discussions.

References

1. H. HAHN AND W. KLINGER, *Z. Anorg. Chem.* **260,** 97 (1949).
2. P. G. RUSTAMOV, P. K. BABAEVA, AND M. R. ALLAZOV, *Russ. J. Inorg. Chem.* **24,** 1223 (1979).
3. P. G. RUSTAMOV, P. K. BABAEVA, D. S. AZHDAROVA, N. A. ASKEROVA, AND M. R. ALLAZOV, *Azerb. Khim. Zh.* **5,** 101 (1984).
4. C. ADENIS, J. OLIVIER-FOURCADE, J. C. JUMAS, AND E. PHILIPPOT, *Rev. Chim. Miner.* **24,** 10 (1987).
5. M. L. ELIDRISSI-MOUBTASSIM, J. OLIVIER-FOURCADE, J. C. JUMAS, M. MAURIN, AND J. SENEGAS, *Hyperfine Interact.* **53,** 317 (1990).
6. R. DIEHL AND R. NITSCHE, *J. Cryst. Growth* **28,** 306 (1975).
7. E. F. BERTAUT, *Bull. Soc. Fr. Minér. Cristallogr.* **79,** 276 (1956).
8. S. L. FINKLEA III, L. CATHEY, AND E. L. AMMA, *Acta Crystallogr. Sect. A: Cryst. Phys. Diffr. Theor. Gen. Crystallogr.* **32,** 529 (1976).

9. L. M. LEVINSON AND D. TREVES, *J. Phys. Chem. Solids* **29,** 2227 (1968).
10. J. R. GOSSELIN, M. G. TOWNSEND, R. J. TREMBLAY, AND A. H. WEBSTER, *Mater. Res. Bull.* **10,** 41 (1975).
11. M. EIBSCHÜTZ, E. HERMON, AND S. SHTRIKMAN, *Solid State Commun.* **5,** 529 (1967).
12. L. BROSSARD, L. GOLDSTEIN, AND M. GUITTARD, *J. Phys.* **37,** C6-493 (1976).
13. E. RIEDEL AND R. KARL, *J. Solid State Chem.* **38,** 40 (1981).
14. R. J. HILL, J. R. CRAIG, AND G. V. GIBBS, *J. Phys. Chem. Solids* **39,** 1105 (1978).
15. G. A. SAWATZKY, F. VAN DER WOUDE, AND A. H. MORRISH, *Phys. Rev.* **183,** 383 (1969).
16. S. HAFNER AND F. LAVES, *Z. Kristallogr.* **115,** 321 (1961).